µb 2001

# RECENT DEVELOPMENTS IN COMPACT STRIP PRODUCTION OF NB-MICROALLOYED STEELS

Karl-Ernst Hensger and Günter Flemming
SMS Demag AG
Eduard-Schloemann-Straße 4
40237 Düsseldorf, Germany

## Abstract

CSP plants process Nb-microalloyed steels into prime-quality hot strip with great reliability. Microalloying provides the prerequisites for a precise setting of the demanded microstructure through thermomechanical rolling. This in turn leads to very favorable material properties. High-strength Nb-microalloyed CSP hot strip is suited for a large variety of applications in mechanical, plant and apparatus engineering as well as in the automotive industry.

## Introduction

Over the past 10 years, the CSP technology has undergone a remarkable development: the materials that are being included into the CSP production program are increasingly ambitious. Today, the CSP product range comprises virtually all material groups that are also processed in integrated steel plants [ 1 ].

One example is the production of high-strength CSP hot strip by means of thermomechanical rolling, also making use of the microalloying technology, in which connection the element niobium is of particular significance.

## Chemical Composition of the Materials Investigated

The chemical composition of the CSP hot strip as investigated meets the demands defined by the relevant European and US standards for hot strip with high yield strength for cold forming, i.e. DIN EN 10149 and ASTM A715-92. The chemical compositions listed in Table I were determined on the basis of these standards, with two aspects particularly taken into account:

Firstly, chemical compositions suitable for setting optimal material properties through thermomechanical processing had to be fixed.

Secondly, optimal conditions for a high CSP process reliability as well as a uniform and reproducible CSP hot strip quality had to be ensured through process-specific narrowing of the tolerances. The scatter bands stated for the different grades can be safely mastered under metallurgical aspects.

Table I shows that for high-strength CSP hot strip of S315MC to S600MC, preference is given to low carbon contents of less than 0.065 %. It is known that the toughness improves and particularly the transition temperature reduces if the carbon content goes down [ 2 ]. At the same time, the surface quality and the welding behavior are positively influenced.

The DIN EN 10 149 standard requires these steels to be „suitable for welding to customary processes". The carbon equivalent CE (IIW) [ 3 ] determined on the basis of the equation as proposed by the International Institute of Welding shows that all relevant prerequisites have indeed been established. For reliable welding without preheating, a CE of less than 0.38 is usually recommended [ 4 ].

For the hot strip grades according to Table I, the growing strength requirements are taken into account by solid-solution hardening primarily through an increasing content of manganese. Moreover there has to be considered that manganese has an austenite-stabilizing effect. Consequently, it reduces the transformation temperature ( $A_{r3}$ ) of the austenite, thereby increasing the ferrite nucleation rate and at the same time reducing the crystal growth rate [ 2 ] – in other words: it has a grain-refining effect.

**Table I Chemical composition of high-strength CSP hot strip with improved formability**

SMS DEMAG

| Steel grade | | Weight % | | | | | | | | ppm | | $CE_{max.}$ (IIW) % |
|---|---|---|---|---|---|---|---|---|---|---|---|---|
| Desig-nation | Material No. | C max. | Mn | Si max. | P, max. | S, max. | $Al_{tot.}$ | Nb | V max. | N | Ca | |
| S315MC | 1.0972 | 0.065 | 0.30<br>0.50 | 0.60 | 0.01 | 0.01 *1 | 0.020<br>0.035 | 0.02<br>0.06 | 0.15 | 40<br>200 | 20<br>40 | 0.15 |
| S355MC | 1.0976 | | 0.70<br>0.90 | | | | | | | | | 0.22 |
| S420MC | 1.0980 | | 1.00<br>1.20 | | | | | | | | | 0.27 |
| S500MC | 1.0982 | | 1.20<br>1.40 | | | | | | | | | 0.30 |
| S550MC | 1.0986 | | 1.40<br>1.60 | | | | | | | | | 0.36 |
| S600MC | 1.8969 | | | | | | | | | | | |

*1 in the present case < 0.005 %

13672E49

The resultant improvement in strength and toughness can be utilized up to approx. 1.6 % Mn.

With silicon, the strengthening coefficient in the ferrite in case of solid-solution hardening is more than twice as high as in case of manganese [ 2 ]. Therefore, the addition of silicon contributes very effectively to a higher yield strength, with the transition temperature, however, being increased thereby, which in turn narrows the margin for alloying with silicon.

Microalloying is playing an important role in the production of high-strength hot strip. It creates, in terms of chemical composition, the prerequisite for thermomechanical processing and pursues 2 goals under the aspect of microstructural formation:

1. Retarding and/or preventing the recrystallization of the hot-worked austenite especially in the late stands of the CSP rolling mill with the aim of setting a substantially fine-grained transformation microstructure

2. Precipitation hardening.

Niobium serves both purposes. It retards quite considerably the recrystallization of the hot-worked austenite already before its precipitation [5]. The hot-work hardening of the austenite thereby attained has a positive impact on the texture and, as a result of subsequent polymorphic transformation, moreover produces a pronounced grain-refining effect [6]. In addition and similar to manganese, niobium dissolved in the solid solution austenite reduces the transformation temperature [7] – which intensifies the grain refinement even further. Therefore, the microalloying technology frequently reacts to growing strength demands by increasing the niobium content [8].

The present study adopted this method for minimum yield strengths up to 500 MPa and niobium contents up to 0.06 %, with the recrystallization-stop temperature ($T_{nr}$) reaching a level enabling sufficient hot-work hardening of the austenite prior to its polymorphic transformation.

The niobium content was not increased further because an excessive increase of the recrystallization-stop temperature would be detrimental to the required recrystallization of the as-cast microstructure in the forward section of the CSP rolling mill.

To attain minimum yield strengths above 500 MPa, microalloying was made with niobium and vanadium. Other than niobium, vanadium does not significantly influence the recrystallization of austenite, but contributes especially to precipitation hardening during and after the $\gamma \rightarrow \alpha$ – transformation.

Maximum-strength steels were specifically nitrided. Nitrogen dissolved in the solid solution has an austenite-stabilizing effect and, in low-carbon steel, promotes the formation of a bainitic microstructure [9]. The increase of the nitrogen fraction in the carbon nitrides of the microalloying elements assists the setting of very fine and uniformly distributed precipitations which raise the strength very effectively [10].

**Fig. 1 Schematic representation of a CSP plant**

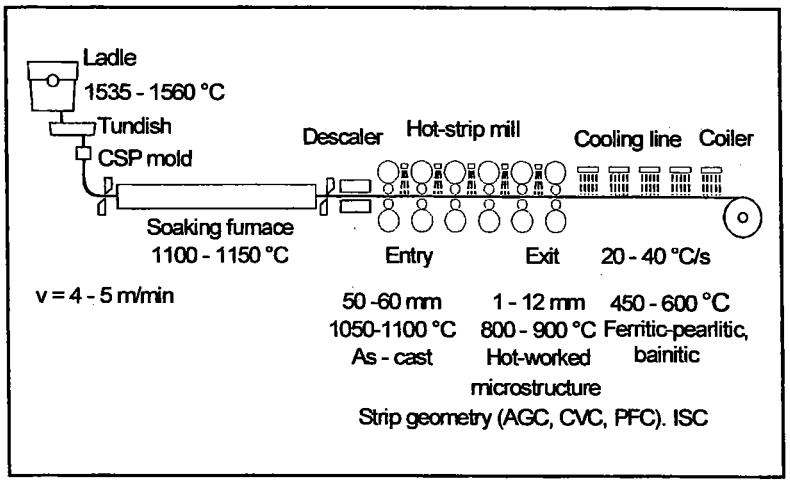


13673E49

## Processing of Nb-microalloyed steels in CSP-plants

Fig. 1 reflects the CSP plant layout and provides information on essential process parameters for the production of microalloyed, high-strength CSP hot strip; plant details can, for instance, be gathered from [11]. The liquid steel is fed via ladle and tundish into the funnel-shaped CSP mold. Leaving the mold, the thin slab runs through to the secondary cooling zone, is cut to length by a pendulum shear and then enters the soaking furnace. After descaling, the slab is rolled in the CSP-HSM; the produced hot strip runs through the laminar cooling system and is finally coiled.

Liquid-steel conditioning and thin-slab casting. All steels investigated here can be furnished via both the converter and the electric arc furnace. In the present case, converter steel was used. An important preparatory step for successful thin-slab casting is a careful secondary-metallurgical

liquid-steel conditioning in the ladle furnace to trim the heat's chemical composition and ensure the demanded chemical and physical homogeneity of the melt.

The content of Al was set to values between 0.020 and 0.035 % (Table I) which harmonizes well with recommendations made in the pertaining literature for preparing melts for thin-slab casting [12]. Higher Al contents are not necessary under deoxidation aspects [13] and, even in conventional continuous casting, lead to a stronger reoxidation tendency and to clogup of the outlets – which are wider there – with aluminates; moreover they have a negative impact on the surface quality.

Setting of the melt's temperature and chemical composition completed, the calcium treatment takes place which pursues two goals:

Under process-technological aspects, it optimizes the castability of the melt thanks to the formation of easy-melting calcium aluminates, and prevents clogging of the submerged entry nozzle (SEN) (see [13, 14]).

The Ca treatment is favorable also from a materials engineering point of view. Instead of MnS which extend in the course of subsequent processing and adversely affect the toughness, oxide sulphides and/or (Ca,Mn)S solid solutions form whose hardness increases so markedly responsive to a growing Ca content that they maintain their quasi-globular shape during the subsequent forming process [13, 14]. This inclusion modification has positive impact on the cold formability, contributes to a higher toughness especially in transverse direction and promotes this way the setting of isotropic material properties.

Following the addition of calcium, soft bubbling was finally effected for approx. 10 min. and with closed slag layer, to enable a substantial precipitation of the inclusions.

With an Al content equal to or below 0.035 %, a sulphur content equal to or below 0.005 % and a calcium level between 20 and 40 ppm as well as with all other casting-technological prerequisites fulfilled, casting in the absence of any troubles was ensured.

An important factor for reliable operation of a thin-slab caster as well as achievement of an unobjectionable surface quality is the selection of an appropriate casting powder. In practice, this selection is often made on the basis of empirical findings. The experience [15] gained in the thin-slab casting of microalloyed steels was summarized in Table II.

For alloying reasons, two different casting powders were used. The ferromanganese adopted led to a carbon charge into the melt not to be neglected. As a result, the recommended carbon content equal to or below 0.065 % was not always met. Due to the fact that, responsive to a growing carbon content, the susceptibility of the strand shell to damage increases, basic casting powder was used instead of acidic powder for steels S550MC and S600MC for preventive reasons.

In the solidified part of the slag film, this measure promotes the formation of crystalline phases which in connection with the pores present there ensure a milder heat removal [16]. This way, a

high process reliability could be ensured in all cases, and surface defects be dependably avoided.

**Table II. Thin slab casting of HSLA grades**

SMS DEMAG

| Steel grade | Casting powder | | Temperature of heat in tundish, $^0$C |
|---|---|---|---|
| | Type | Basicity | |
| S315MC<br>S355MC<br>S420MC<br>S500MC | A | 0.9 | 1540 - 1560 |
| S550MC<br>S600MC | B | 1.17 | 1535 - 1555 |

| | |
|---|---|
| Powder consumption: | 0.08 - 0.10 kg/m² |
| Elektromagnetic brake: | aktiviert |
| Casting speed: | 4 - 5 m/min: |
| Temperature on slab surface ahead of shear: | ≥ 1000 °C |
| Slab width: | 900 - 1600 mm |
| Slab thickness: | 50 mm |

13676E49

The level and width of the temperature window in the melt to be met are in a close correlation with the thermophysical properties of the casting powder used. Uniform melting of the powder and reliable drawing-in of the formed slag film into the casting gap between strand shell and mold in particular must be ensured [17].

For the data according to Table II, operation with electromagnetic brake (EMBr) was presupposed. With the EMBr deactivated, the flux pattern of the melt inside the mold changes and so does the temperature in the meniscus area. In that case, the recommended temperature window has to be corrected upwardly by approx. 5 $^0$C.

Owing to the favorable impact on the homogeneity of the slab, the plant was run with soft reduction in the area of the solidification point. The casting speed ranged between 4 and 5 m/min.

For the behavior of Nb-microalloyed thin slabs, it is of utmost importance that an adequately high strand temperature be met in the area of the secondary cooling line.

The microalloying elements are able to fulfil their process-technological goals in the rolling mill and the laminar-flow cooling line only when they are kept in the state of solid solution in the area of the caster.

Premature precipitation of Nb(C,N) in the area of the secondary cooling line reduces the content of the microalloying element in the solid solution that is available for the intended setting of the microstructure in the rolling mill and the laminar cooling line. Moreover, the risk of hot embrittlement and formation of transversal cracks in the strand grows [18].

In the present case it was therefore ensured by way of controlled width-dependent cooling-water dosing as well as air-mist cooling that the temperature of the slab – before running into the soaking furnace – did not drop below 1000 - 1050 $^0$C even in the area of the edges (slab center: 1080 $^0$C).

Temperature equalization in the roller-hearth furnace and thermomechanical rolling with direct charging. Having left the caster, the slab runs through a roller-hearth furnace for temperature equalization over its thickness, width and length. For the materials described here, the furnace was set to 1100 to 1150 $^0$C, which relatively high equalization temperature ensures that niobium remains completely dissolved in the solid solution also in the area of the soaking furnace.

The central concern of thermomechanical processing (TMP) is the specific utilization of plastic deformation beyond the forming work as such to control solid-state reactions and to set defined microstructures with specified physical material properties [19]. The work-hardening and softening processes taking place in the rolling mill are markedly modified through microalloying with niobium (Fig. 2). Plain unalloyed steels, owing to the fact that they fully recrystallize between the passes, feature a low flow stress during hot forming.

**Fig. 2 Material response on microstructure changes in CSP – HSM (Scheme)**

SMS DEMAG

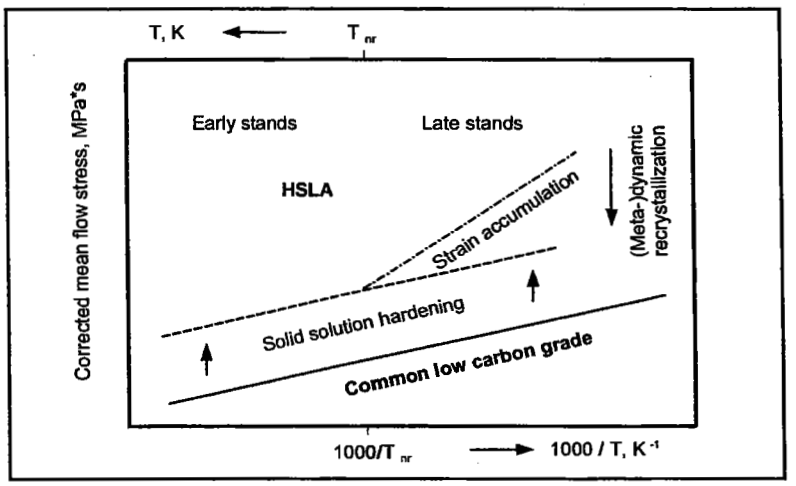


Solid-solution hardening increases the flow stress. In addition, niobium leads to a higher recrystallization stop temperature $T_{nr}$. When the rolling temperature drops below this value, the result is an accumulation of strain and an increase of the flow stress due to the incomplete recrystallization between successive passes [20]. This may finally trigger dynamic and metadynamic recrystallization, with a reduction of the flow stress for consequence. Deformation-induced precipitations may occur as well. All of these processes of microstructural formation can be implemented for Nb-microalloyed steels in the CSP rolling mill. By using the available high-performance process control, the microstructure of the hot-formed austenite is precisely set this way.

Successful thermomechanical processing calls for essential CSP-process-specific characteristics to be observed (Table III):

1. The thin slab is always rolled after direct charging, austenitization taking place through $\delta \rightarrow \gamma$- transformation during cooling of the solidified strand. Therefore, the austenitizing temperature is very high and the present austenite grain very coarse. A coarse austenite grain has a recrystallization-retarding effect.

2. The slab running into the CSP rolling mill has an as-cast microstructure.

**Table III. Thermomechanical processing on CSP plants** SMS DEMAG

1. Direct charging

2. A thin-slab with as-cast microstructure enters the CSP-HSM

$$\varepsilon_R + \varepsilon_C \rightarrow \varepsilon_\Sigma$$

approx. 60 % ≥ 60 ... 70 % ≥ 80 %

| Slab thickness, mm | Thickness of "roughed" slab, mm | Maximal hot strip gage, mm |
|---|---|---|
| 50 | 25 | 7.5 - 10 |
| 60 | 30 | 9 - 12 |
| 70 | 35 | |

13677aE49

Under materials engineering aspects, the rolling mill has to fulfil two tasks:

Firstly, the dendritic as-cast microstructure has to be compacted and transformed into a homogeneous, recrystallized microstructure. To solve this task, the partial deformation $\varepsilon_R$ is available at temperatures of $T > T_{nr}$.

Secondly, the austenite has to be conditioned to attain the thermomechanical processing effect. To this end, the partial deformation $\varepsilon_C$ has to be applied at temperatures of $T < T_{nr}$.

To successfully solve both tasks, adequate constitutional and rolling-technological prerequisites have to be established. From a constitutional standpoint, microalloying deserves particular attention. By selecting the niobium content the recrystallization stop temperature is set. On the one hand, the content of niobium must not be too high so as to ensure smooth and complete recrystallization of the as-cast microstructure in the early part of the CSP-HSM. On the other hand, the content of niobium must be so high that the desired hot-work hardening of the austenite in the late stands is ensured (also see Fig. 2). Selection of the pass schedule enables an efficient distribution of the total deformation among the individual stands and hence also

| mm | $e_R$ | $e_C$ 60% | $e_C$ 70% |
|---|---|---|---|
| 50 | 25 (50%) | 10 | 7.5 |
| 60 | 30 (50%) | 12 | 9.0 |
| 70 | 35 (50%) | 14 | 10.5 |

among the temperature ranges of complete and incomplete recrystallization. The information and data in Table III may serve as a guideline.

To ensure complete static recrystallization between the first passes, the material is entered into the CSP rolling mill at high temperatures (1060 – 1080 $^0$C) and, other than in conventional roughing mills, is rolled with a high reduction equal to or above 50 % already in the first stand. Moreover, softening can be accelerated by initiating dynamic recrystallization. Fig. 3 shows that referred to an initial grain size of 1000 µm, the critical strain for dynamic recrystallization at 1080 $^0$C is approx. 55%.

Metadynamic recrystallization which takes place right after dynamic recrystallization without any incubation period is a very quick process and completed before the end of the inter-pass time.

**Fig. 3 Effect of temperature and grain size on the critical reduction for DRX**

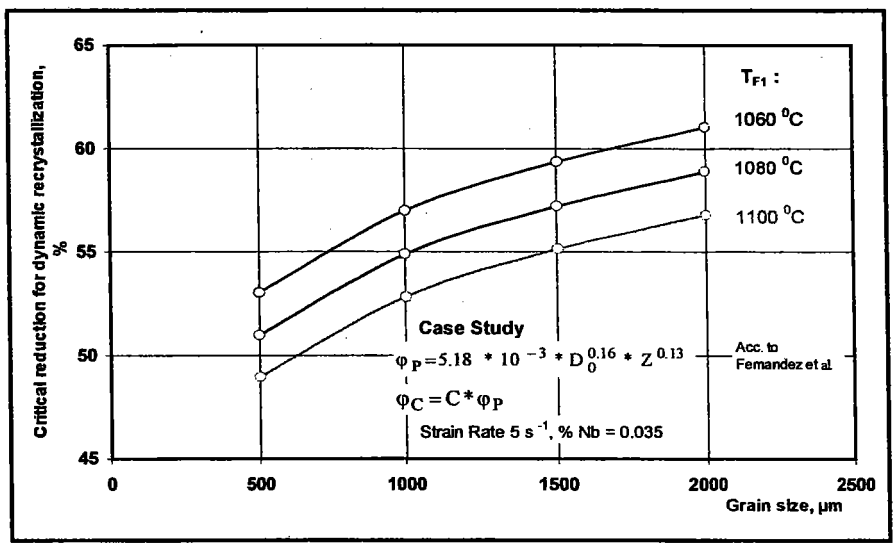


S1+W4-13999E

This means that the material is completely softened, homogeneous and recrystallized before entering the next stand.

In the rear part of the rolling mill it is typical of Nb-microalloyed hot strip that the temperature drops below the recrystallization stop temperature ($T_{nr}$), which means that the static recrystallization between the stands remains incomplete so that more and more strain accumulates from one pass to the next (also see Fig. 2).

These findings correspond with texture measurements. Following hot rolling and transformation in the bainitic microstructure, the texture was measured on the residual austenite (for details of method see [22]).

Although the full EULER-space that applies to rolled austenite covers the range $0 < \varphi_1 < \pi/2$, $0 < \Phi < \pi/2$, $0 < \varphi_2 < \pi/2$, nearly all orientations that are of interest to steel processing can be found along the so-called α- and β-fibers - Fig. 4 [23]. The α-fiber runs from the GOSS to the brass orientation, i.e. from {011}<100> ... {011}<211>. The β-fiber ranges from the copper via the S to the brass orientation, i.e. from {211}<111> ... {123}<634> ... {011}<211>.

**Fig. 4 Main texture components in flat rolled fcc metals (Austenite)**

SMS DEMAG

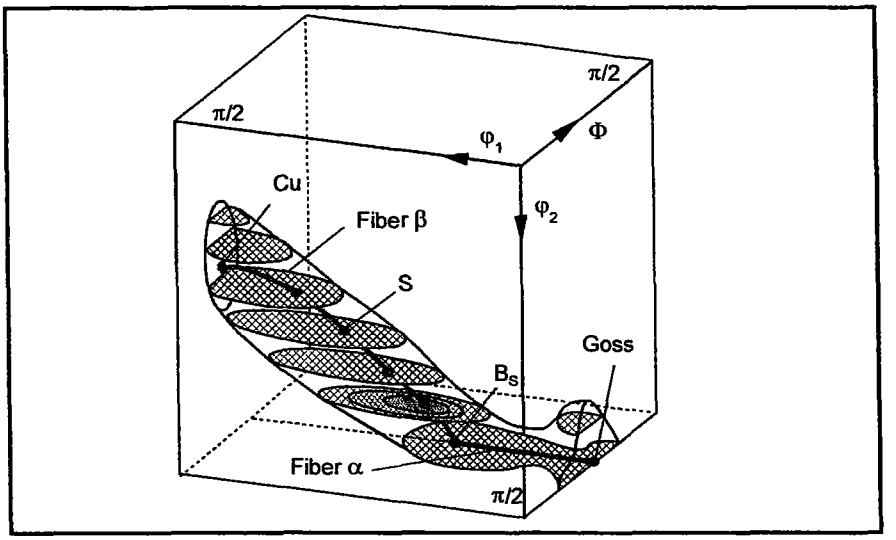


S1+W4-14000E

The developed intensities of these principal components depend on the strain that can be accumulated without recrystallization as well as on the stacking fault energy.

Fig. 5 reflects the intensities along the α- and β-fibers for the hot-worked (residual) austenite of S550MC [22]:

The α–fiber consists of {011}<uvw> orientations where the {011} planes lie in the rolling plane and are therefore perpendicular to the normal direction ND. The highest intensity is found near the brass orientation {011}<211> (approx. 17 times higher than in case of random orientation); the GOSS orientation {011}<100> features a 9-times greater intensity than in case of random orientation.

Again recognizable in the β-fiber is the very pronounced brass orientation (also see Fig. 4) and next to it the copper orientation {112}<111> with an 8-times greater intensity than in case of random orientation.

**Fig. 5 α– and β–fibers in S550MC**

SMS DEMAG

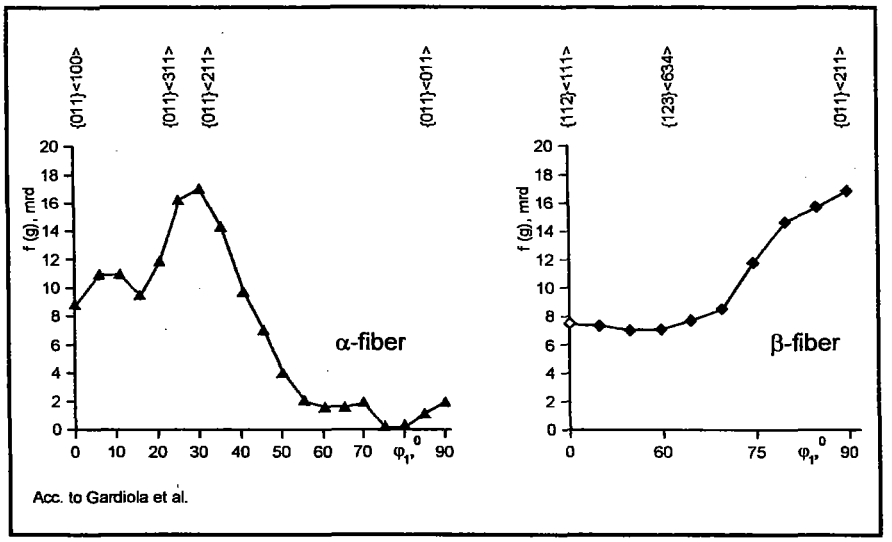


S1+W4-14001E

When, for comparison, defining a fiber for which RD // <110> applies (so-called RD fiber), then one finds that besides the mentioned as-rolled orientations a cube orientation (9-times more intensive than in case of random orientation) also occurs.

The formation of cube orientation is connected with the recrystallization of the austenite in the early part of the CSP rolling mill. The formation of as-rolled orientations is due to the effect of the microalloying element niobium which enables great strain to accumulate in the rear part of the mill: own model calculations which corresponded well with model tests [24] showed accumulated strains of approx. 1.2 (approx. 70 %) after finish rolling. This explains that in the present case typical as-rolled orientations with great intensity dominate the texture of the hot-worked (residual) austenite. The setting of these preferred orientations in the austenite has a favorable impact on the material properties after polymorphic transformation (see later in this paper).

Niobium can be present in dissolved form in the solid solution austenite or precipitated as carbon nitride. When dissolved in the solid solution, niobium retards the recrystallization of the hot-worked austenite, while niobium in the form of precipitations stops the recrystallization. For rolling heavy plates it is considered typical that Nb-precipitations form, thereby leading to the so-called pancaking of the austenite grains. When rolling hot strip, niobium typically is left in the solid solution. While in the first case the longer retention time of the material in the rolling mill favors precipitations, that time is, as a rule, not long enough in continuous hot strip mills to allow precipitations to form. There are, however, exceptions from this rule [25]. As the precipitation of niobium from the solid solution drastically changes the behavior of the material, this situation was investigated also for a CSP rolling mill.

**Fig. 6 Comparison between precipitation start curve and CSP-HSM cooling curve**

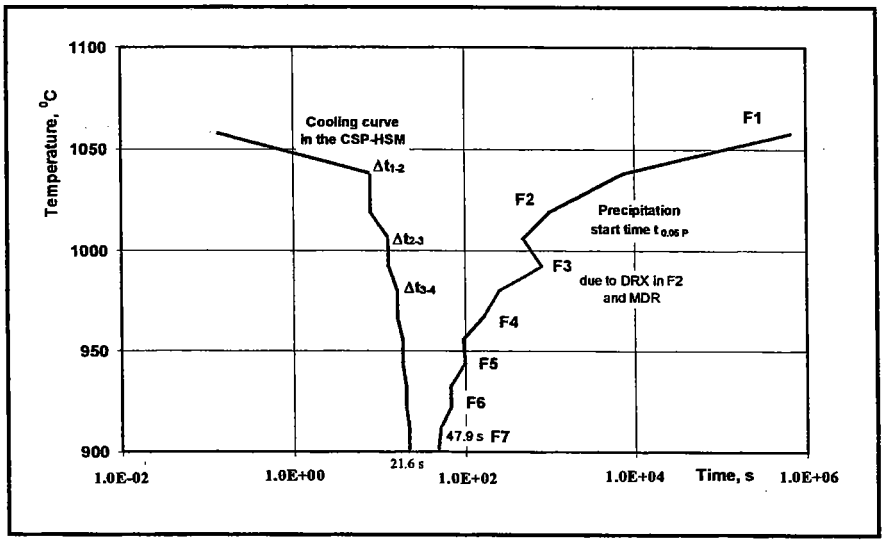


S1+W4-14003E

The methods employed are based on studies by Dutta and Sellars [26] as well as Jonas [27], also using Scheil's additivity rule [28]. The results of the calculations can be seen from Fig. 6.

The continuous cooling curve of the material in the finishing mill was discretized. Calculated then was the incubation time for the precipitation of Nb(CN) for the individual temperature levels under the impact of the accumulated strain existing there. The criterion for the deformation-induced precipitation is the contact of both curves. One can see that, under given conditions, there are no Nb(CN) precipitations in the CSP rolling mill – the incubation time considerably exceeds the time the strip is in the CSP rolling mill.

Laminar cooling and coiling. Polymorphic transformation of the austenite that was previously hot-worked in the CSP rolling mill takes place in the laminar cooling line; it is here and on the coiler that the final microstructure is set.

There is a close correlation between the ferrite grain size that forms, the strain accumulated in the rolling mill, the austenite grain size and the cooling rate on the roller table (see equation in Fig. 7) which can be used for microstructural modeling. For example: with a residual deformation of 0.8, an austenite grain size of 20 µm and an average cooling rate of 25 $^{0}$C/s, a ferrite grain size of approx. 5 µm is calculated. This corresponds well with the results obtained from experiments (see Fig. 9).

An as early and as intensive as possible cooling from finish-rolling to coiling temperature allows the lattice defects produced as a result of hot deformation to be utilized most completely for impacting the polymorphic transformation – such a cooling strategy intensifies the attainable grain refining effect [30].

**Fig. 7 Grain refinement due to polymorphic transformation** SMS DEMAG

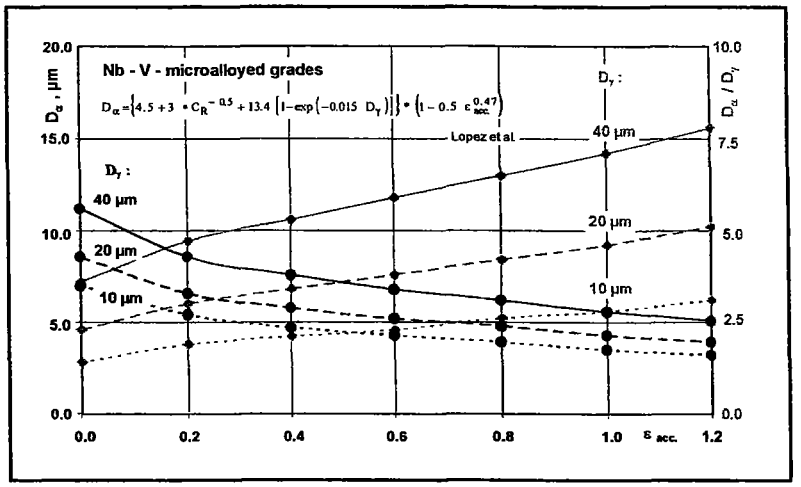


S1+W4-14004E

Fig. 8 shows cooling curves implemented for 6-mm-thick CSP hot strip of S550CM (strip middle and center). One recognizes that the coiling temperature is reached very quickly (early quick mode), whereby the fraction of almost isothermally transformed austenite increases which in turn promotes the homogenization of the transformation microstructure. The average cooling rate from finish-rolling to coiling temperature ranges between 25 – 40 $^0$C / s.

**Fig. 8 Cooling curves for the middle of CSP hot strip (gage 6 mm, grade S550MC)** SMS DEMAG

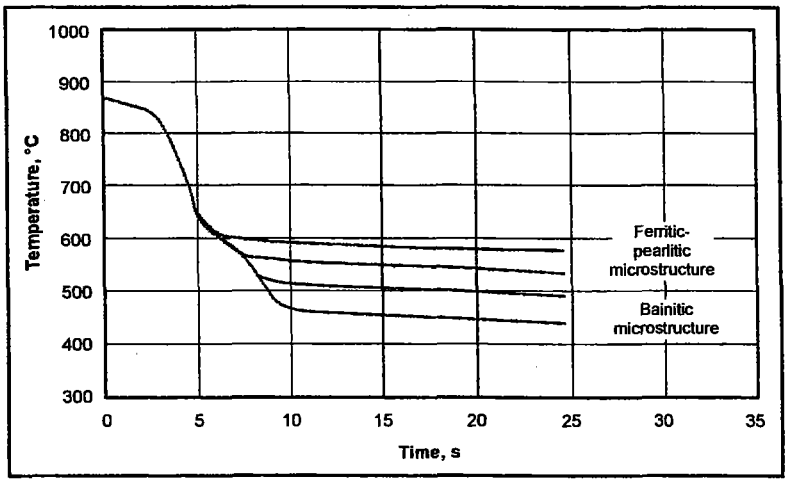


13679E49

The TTT (ε) diagrams available in the literature indicate that, under these conditions, a ferritic-pearlitic microstructure forms between 500 and 600 $^0$C and a bainitic microstructure at temperatures below 500 $^0$C [30]. A lower coiling temperature moreover contributes to a refining of the precipitations that form.

of this technology can be utilized for microalloyed, high-strength CSP hot strip for improving the material refinement and/or for reducing the production cost. A higher level of material refinement can be achieved through more intensive grain refining, greater precipitation hardening and the controlled setting of non-equilibrium microstructures, while the cost can be cut by saving alloying elements.

## Microstructure and Properties of High-Strength CSP Hot Strip

Characterization of microstructure and submicrostructure. Fig. 9 reflects selected micrographs of CSP hot strip here investigated (gage: 8 mm). Grades S315CM and S420CM were finish-rolled at 900 $^0$C and coiled at 580 and/or 570 $^0$C. For setting a greater strength, steel grade S550CM was finish-rolled at a lower temperature of 850 $^0$C and coiled at an approx. 80 - 100 $^0$C lower temperature.

**Fig. 9 Microstructure of high-strength microalloyed CSP hot strip**

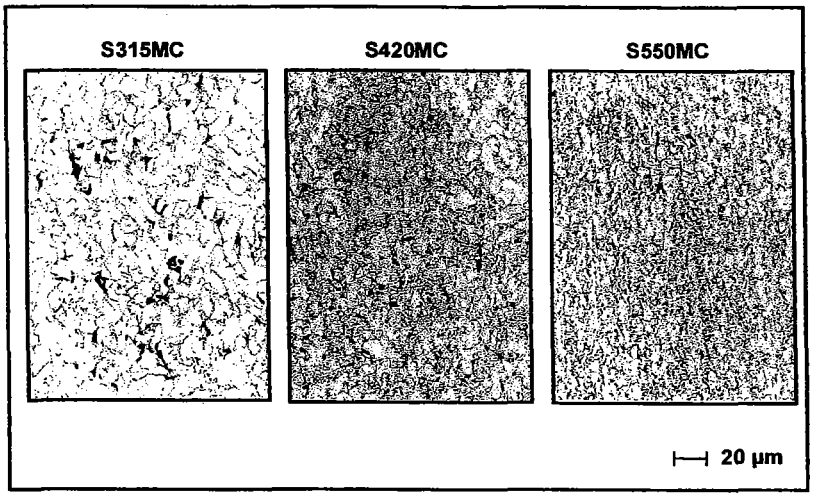


With increasing strength class, a growing grain refinement is noticed: the average ferrite grain size in CSP hot strip of S315CM is approx. 6 µm (grain-size number 12 – 11), that of S550CM approx. 4 - 5 µm (grain-size number 13).

As far as S315MC and S420MC are concerned, we have a ferritic-pearlitic microstructure. The dark-etched pearlite is located at the ferrite grain boundaries. Owing to the higher manganese content, it is finer for S420MC than for S315MC. In CSP hot strip of S550MC, the selected chemical composition and the markedly lower coiling temperature lead to the formation of a bainitic microstructure.

As regards bainitic microstructures, one expects lath- or plate-shaped ferrite crystals, the so-called acicular ferrite [32]. There has to be considered, however, that the bainitic microstructure

**Fig. 10 Grain-size distribution and properties of CSP hot strip: S550MC**

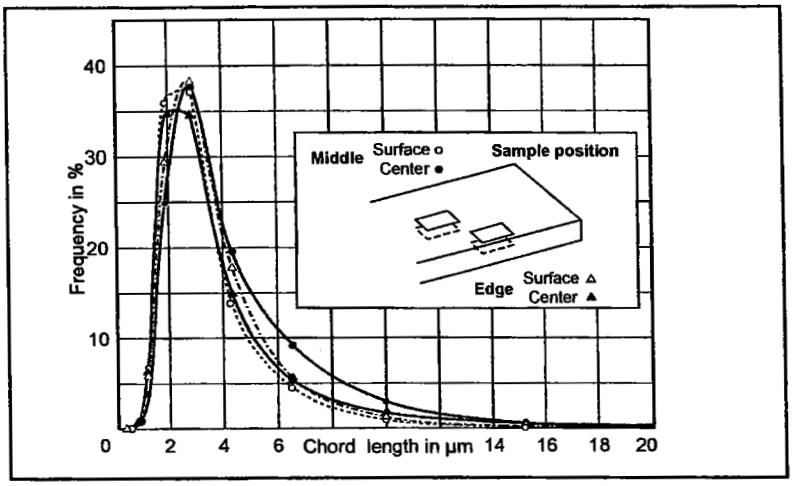


13681E49

of low-carbon microalloyed steels reacts to the thermomechanical history. An increasing hot-work hardening of the austenite causes the morphology of bainite to change from acicular to quasi-globular [30, 35]. The ferrite grains observed are just slightly stretched in rolling direction (Fig. 9 – S550MC).

**Fig. 11 TEM Characterization of substructure in CSP hot strip (grade S550MC)**

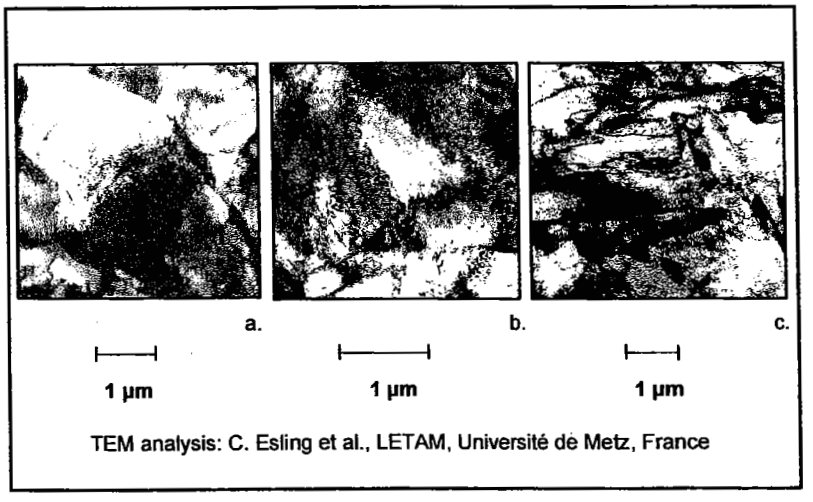


13682E49

Fig. 10 reflects the grain-size distribution curves for different locations in CSP hot strip of S550MC, i.e. at the edge and in the middle of the strip, on the strip surface and in strip center (core). All grain-size distribution curves are nearly identical, evidencing the great homogeneity of the transformation microstructure in the hot strip.

Transmission-electron-microscopic investigations revealed different ferrite fractions in the transformation microstructure of CSP hot strip of S550CM (Fig. 11):

Fraction I consists of nearly globular ferrite grains, approx. 2-4 µm in size, featuring a low dislocation density (Part Figure a).

Typical of fraction II are smaller ferrite crystals (approx. 0.5 µm) with a higher dislocation density. The dislocations tend to form cells (Part Figure b).

In fraction III, lath-shaped ferrite crystals with a high dislocation density are arranged in(to) packs which consist of up to 5 laths and are slightly stretched in the direction of the lath-shaped ferrite crystals. The individual laths are 1 – 4 µm long and 0.1 – 0.5 µm wide. Within one pack, the ferrite crystals exhibit almost the same crystallographic orientation – the boundaries between them are subboundaries. By contrast, different packs feature different crystallographic orientations; the pack boundaries are large-angle grain boundaries.

The coexisistence of different microstructural fractions is the result of transformation during continuous cooling [32]. Cementite or pearlite were discovered neither transcrystalline nor intercrystalline. Coarse carbides were not found either. The precipitations were very small (a few nm). They were finely dispersed in the ferritic matrix and were identified as Nb(CN). Owing to the insufficient size, the diffraction pattern appeared very diffuse; therefore, it was not possible to precisely determine the lattice parameters.

**Fig. 12 RD- and TD-fibers in S550MC**

SMS DEMAG

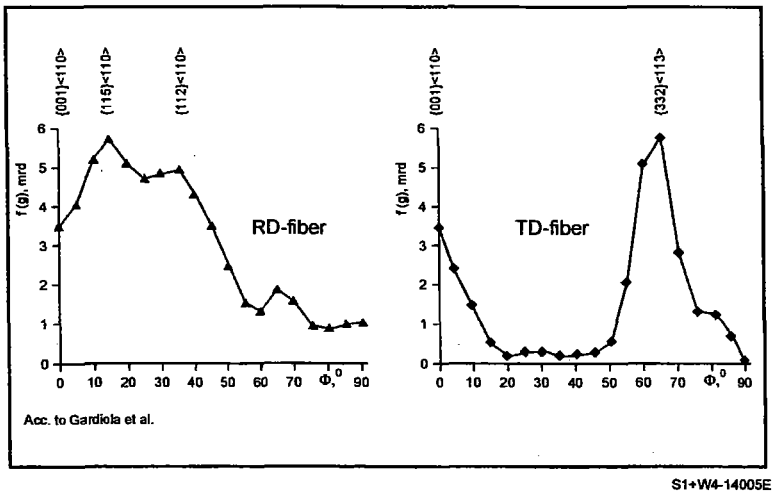


S1+W4-14005E

The microstructure was further characterized by way of X-ray texture investigations. Similar to the austenite texture, the ferrite texture, too, can be described by means of main texture fibers.

The so-called RD-fiber consists of crystallographic orientations which are characterized by the fact that their <110> directions run parallel to the RD, i.e. it consists of {hkl}<110> orientations.

The TD-fiber features orientations whose <110> directions run parallel to the TD.

Fig. 12 depicts the RD- and the TD-fiber of the ferrite texture as well as the main orientations:

The RD-fiber exhibits two maxima near the orientations {115}<110> ... {112}<110>; the intensity is 5- to 6-times greater than in case of random orientation. In addition, there is one maximum near the orientation {001}<110>, the intensity being 3.5-times higher than in case of random orientation.

In the TD-fiber, there is a distinct maximum near the orientation {332}<113>, the intensity being 6- to 7-times higher than in case of random orientation; additionally, one can again see the orientation {001}<110>.

Further to these measurements, the ferrite texture was also calculated on the basis of the austenite texture using the orientation relationships according to Nishiyama-Wassermann and Krudjumov-Sachs (without variant selection). This calculation produced the following results:

The main components of the RD-fiber are connected with the Cu-orientation and the main orientation of the TD-fiber with the brass orientation of the austenite. The weaker orientation {001}<110> is the result of transformation of the cube orientation.

Microalloying with niobium leads during thermomechanical rolling to a severe hot-work hardening of the austenite as well as to an adequately intensive transformation texture in the ferrite. The orientations resulting from the as-rolled orientations of the austenite dominate the ferrite texture.

Niobium suppresses the recrystallization of the austenite and the involved formation of the cube orientation. The {001}<110> resulting from the cube orientation of the austenite is therefore relatively weak, which contributes to an increase in toughness. If this orientation is more pronounced, then this is assumed to be in connection with a probable delamination in case of impact stress [34].

The results of the investigations into the microstructure show that during TMP all mechanisms available for increasing the strength are utilized. Solid solution hardening and grain refinement, precipitation hardening, and the increase of the dislocation density as a result of the bainitic transformation altogether contribute to the manufacture of high-strength CSP hot strip.

Material properties. Figures 13 to 15 illustrate the impact that important CSP process parameters have on the attainable mechanical properties with reference to steel grade S550MC.

Fig. 13 Influence of rolling temperature in the first stand on the yield strength (grade S550MC)

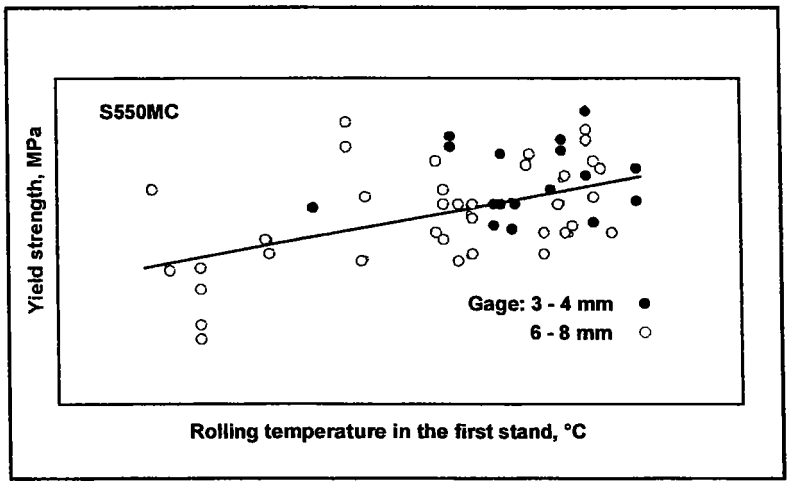


Fig. 13 shows that the yield strength attainable for CSP hot strip of S550MC rises when the entry temperature goes up. An increase of the entry temperature from approx. 1050 to 1100 $^0$C allows to raise the yield strength by approx. 50 MPa. This temperature increase ensures that the available niobium is present in the solid solution when the thin slab runs into the rolling mill. With decreasing slab temperature, the precipitation tendency of Nb(CN) intensifies prior to

Fig. 14 Influence of the finishing temperature on the yield strength (grade S550MC)

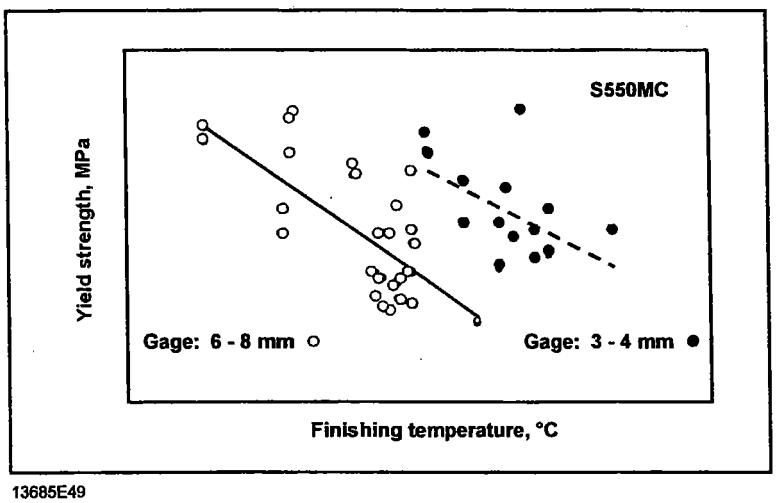


rolling, this having a negative impact on the final properties. It is obvious that the dependence of the attainable yield strength on the entry temperature does not depend on the finished-strip thickness; in other words: the material should be entered at as high a temperature as possible irrespective of the demanded strip thickness. It is, however, also apparent that a high starting temperature alone is no guarantee for achieving the demanded minimum yield strength. The results presented in the following provide closer details in this regard.

The influence of the finish-rolling temperature on the achievable yield strength is illustrated in Fig. 14. The yield strength goes up when the finish-rolling temperature goes down, reason being that a higher finish-rolling temperature leads to increased hot-work hardening of the austenite along with a greater refinement of the microstructure after polymorphic transformation [6].

To achieve the same yield strengths, a thicker finished strip must be finish-rolled at lower temperatures, because the strain available for conditioning the austenite prior to its transformation reduces when the strip thickness goes up. This effect is compensated by reducing the finish-rolling temperature.

In the present case, a 6 - 8-mm-thick strip of S550CM must definitely be finish-rolled at temperatures equal to or below 850 $^0$C to achieve the demanded yield strength of 550 MPa. Thinner strips attain this value even at finish-rolling temperatures of 885 $^0$C.

**Fig.15 Influence of coiling temperature on the yield strength (grade S550MC)**

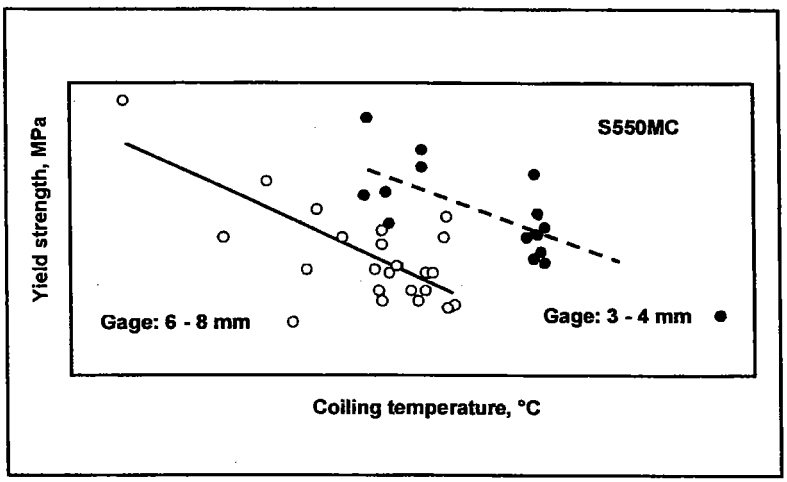


As can be seen from Fig. 15, the attainable yield strength goes up as the coiling temperature decreases. A reduced coiling temperature shifts the transformation of the hot-worked austenite towards lower temperatures. The bainitic microstructure which forms is finer, its dislocation density is higher and smaller precipitations form, with a greater strength for consequence.

Heavier-gage hot strip cools more slowly. Consequently, when the hot-strip thickness reduces, transformation starts at a higher temperature, which - under otherwise identical conditions - leads to strength losses. This effect can be counteracted by reducing the coiling temperature. In the case under investigation one can see that for 3 – 4-mm-thick hot strip of S550MC yield strengths over 550 MPa are set at coiling temperatures equal to or below 550 $^0$C. To attain the same result for a 6 – 8-mm-thick product, a coiling temperature between 450 and 480 $^0$C must be adhered to.

The results presented demonstrate that an adequately wide technological window is available for reliably setting the demanded minimum yield strength. The available process-technological scope enables efficient process control and ensures great process reliability.

**Fig. 16 Mechanical properties of microalloyed CSP hot strip**

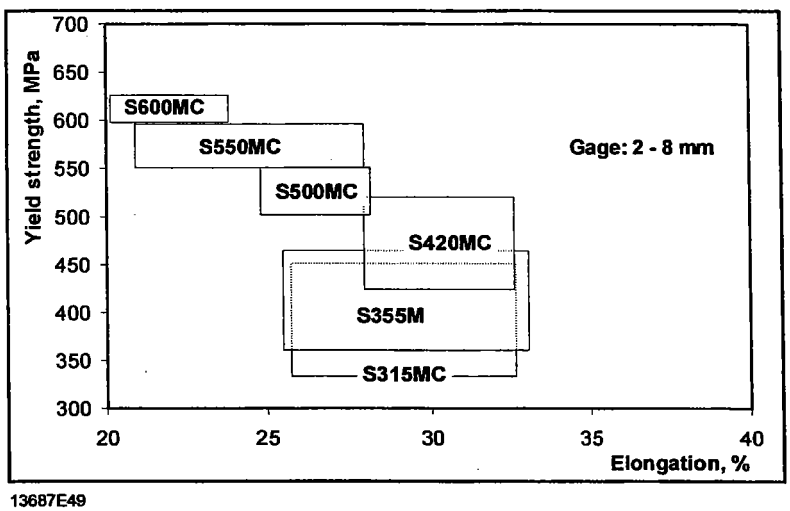


Further to the demanded yield strength, the hot-strip grades investigated allow defined minimum elongations to fracture to be attained, these ranging between 24 % for S315MC and 13 % for S600MC (nominal thickness ≥ 3 mm). Fig. 16 illustrates in summarized form for all grades examined here that the demanded elongations to fracture were not only reliably achieved, but even markedly exceeded.

Bending tests carried out in addition to the tensile test produced altogether positive results; no failure occurred.

Fig. 17 depicts the temperature dependence of the notch impact energy for CSP hot strip of S550CM. Tested were 5*10 $mm^2$ longitudinal and transversal samples in Charpy arrangement. The toughness values ascertained reliably meet the requirements acc. to the DIN EN 10 149 standard. The transition temperature from ductile fracture to brittle fracture is –50 $^0$C: CSP hot strip features an excellent combination of strength and toughness.

It was thus evidenced that adopting thermomechanical processing in the production of CSP hot strip allows to attain high strength along with excellent plasticity and toughness. Ensuring an exacting combination of strength and toughness is the prerequisite for successful application of these high-strength microalloyed strips in multifarious fields.

Applications: the very good material properties evidenced by means of mechanical test methods were fully confirmed by the favorable processing and service behavior of the CSP hot strips. The users of high-strength hot strip come from different industrial branches, for instance

**Fig. 17 Effect of test temperature on the impact energy of CSP hot strip S550MC**

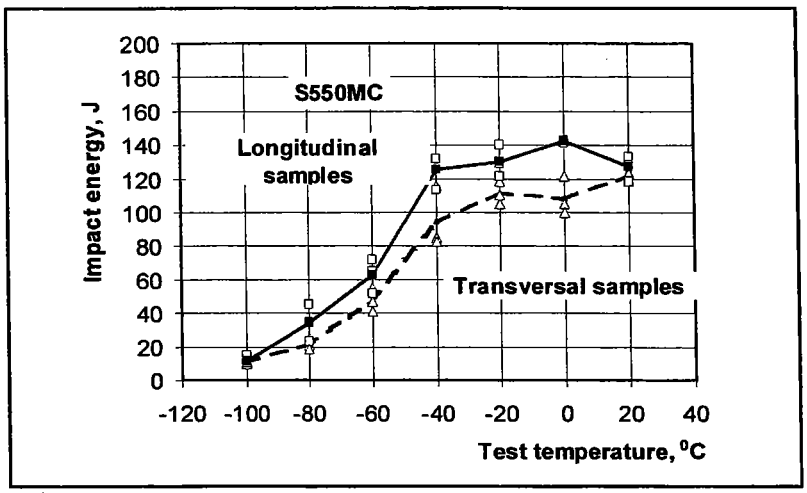


13688E49

machine, apparatus and plant building as well as the automotive industry. A wide spectrum of products was manufactured (Table IV) all of which have proved successful in and suitable for a great variety of applications.

**Table IV. Examples of application for high-strength CSP hot strip**

| Steel grade | Application of hot strip |
|---|---|
| S315MC | Construction of machinery: grippers for agricultural pickers, strapping material |
| S420MC | Construction of apparatus and appliances: pressure tanks |
| S500MC | Car construction: door internals, skid rails, spring housings, wheel rims, wheel guides |
| S550MC | Plant construction: conveyors, cranes, scaffolders, warehousing and shelf elements |

13689E49

With its processing and service behavior proved to be equal, CSP hot strip represents an attractive alternative to conventionally produced high-strength hot strip, not least thanks to the considerable cost benefits it offers.

## Conclusions

The controlled adoption of metallurgical action principles along with the consideration of specific aspects of the CSP process enable Nb-microalloyed hot strip to be produced on CSP plants with great process reliability. The products meet the European and US standards for high-strength hot strip intended for cold forming.

Thermomechanical processing allows to set a very high ductility in addition to high strength even at low temperatures. The correlations established for thermomechanical rolling in CSP plants between process-technological parameters and the microstructure and material properties correspond well with results obtained in conventional rolling mills.

In terms of quality, CSP hot strip is equivalent to hot strip produced the conventional way. It is used for a large variety of applications in machine, plant and apparatus building as well as in the automotive industry.

## References

1. G. Flemming, K.-E. Hensger: „Present and future CSP technology expands product range", AISE Steel Technology, Jan. 2000, 53-57

2. T. Gladman, The Physical Metallurgy of Microalloyed Steels, The Institute of Materials, 1997

3. S. Liu,"Weldability of Steels", Metals Handbook, 10th Ed., 1990, vol. 1, 603 – 613

4. C. Shiga, „Benefits of TMCP and its application to HSLA steels", Metallography`95, 195-200

5. M.G. Akben, I. Weiss, J.J.Jonas, „Dynamic Precipitation and Solute Hardening in a V Microalloyed and Two Nb Steels Containing High Levels of Mn", Acta Metallurgica, 29, (1981), 111-121

6. L.J. Cuddy, „Grain Refinement of Nb-Steels by Control of Recrystallization During Hot Rolling", Metall. Trans. 15A, (1984), 87-98

7. L.E. Collins, D.L. Baragar, J.T. Bowker, „Steckel Mill Process Optimization for Production of X70 and X80 Gas Transmission Linepipe", Microalloying `95, 1995, 141 - 147

8. K. Hulka, „Alloy Design, Processing and Application of High Strength Steels", Metallurgy and New Materials, 1995, No. 3, 1 – 22

9. M.P. Staiger, B. Jessop, P.D. Hodgson, A. Brownrigg, C.H. Davies, „Effect of Nitrogen on Formation of Martensite-Austenite Constituent in Low Carbon Steel", ISIJ Intern., 39, (1999), 183-190

10. S. Zajac, R. Lagneborg, T. Siwecki, „The Role of Nitrogen in Microalloyed Steels", Microalloying `95, Conference Proceedings 1995, 321-338

11. G. Kneppe, D. Rosenthal, „Warmbandproduktion: Herausforderungen für das neue Jahrtausend", Stahl und Eisen, 1998, Nr.7, 61-68

12. J.K. Brimacombe, I.V. Smarasekera, „The Callanges of Thin Slab Casting", Near Net Shape Casting in the Minimills", Proc. of the Int. Symp., Vancouver, BC, Canada, 1995, Aug., 19-23

13. K.-H. Heinen, Elektrostahlerzeugung, Düsseldorf, Verlag Stahleisen 1997

14. K. Tönshof, W. Kaestner, R. Schnadt, „Metallurgische Auswirkungen der Ca-Behandlung von Stahlschmelzen auf das Stranggießen", Stahl und Eisen 109, (1989), Nr. 16, 743

15. M. Kolakowski, Pers. Information, 1996

16. K.C. Mills, „Mould Fluxes for Contiuous Casting and Their Effect on Product Quality", McLean Symp. Proceedings 1998, 195-201

17. S.L. Wigman, M.D. Millet, „Demands on Refining Processes in Thin Slab Casting", Scaninject VI: 6th Int. Conf. on Refining Processes. Lulea, Sweden 1992, 1-17

18. N. Banneberg, N., B. Bergmann, H.-A. Jungblut, N. Müller, K. Reich, „Procedures for Successful Continuous Casting of Steel Microalloyed with Nb, V, Ti, and N", Microalloying `95, 1995, pp. 83-94

19. K.-E. Hensger, M.L. Bernstein: Thermomechanische Veredlung von Stahl, Leipzig, Deutscher Verlag für Grundstoffindustrie, 1984

20. D.Q. Bai, S. Yue, T. Maccagno, J.J.Jonas, „Static Recrystallization of Nb and Nb-B Steels under Continuous Cooling Conditions", ISIJ Intern., 36, (1996), N8, 1084-1093

21. A.I. Fernandez, R. Abad, B. Lopez, J.M. Rodriguez-Ibabe, „Effect of Coarse Grain Size on the Dynamic and Static Recrystallization during Hot Working in Microalloyed Nb and Nb-Ti Steels", Materials Science Forum, 284-286, (1998), 135-142

22. B. Gardiola, M. Humbert, C. Esling, G. Flemming, K.-E. Hensger, „Determination and prediction of the inherited ferrite texture in a HSLA steel produced by compact strip production", Materials Science and Engineering, A303, (2001), 60-69

23. J.J. Jonas, „Effect of processing parameters on texture and anisotropy of high performance steels", Proc. of the 7th Intern. Conf. on steel rolling, 1998, 9-11.Nov., 524-533

24. D. Luo, P. Zeng, „Influence of the accumulated residual strain on deformation resistance and static softness during hot rolling Nb, V bearing HSLA steel", Iron and Steel, 31, (1996), Nr. 1, 49-53

25. K. Minami, F. Siciliano, T.M. Maccagno, J.J. Jonas, „Mathematical Modeling of Mean Flow Stress during Hot Strip Rolling of Nb Steels", ISIJ Intern., 36, (1996), N.12, 1507-1515

26. B. Dutta, C.M. Sellars, „Effect of composition and process variables on Nb(C,N) precipitation in niobium microalloyed austenite", Mat. Sci. And Tech., 3, (1987), 197-206

27. L.N. Pussegoda, P.D. Hodgson, J.J. Jonas, „Design od dynamic recrystallization controlled rolling schedules for seamless tube rolling", Mat. Sc. And Techn., 8 (1992), 63- 71

28. E. Scheil, „Anlaufzeit der Austenitumwandlung", Arch. f. d. Eisenhüttenw., 12, (1935), 565-567

29. R. Bengochea, B. Lopez, I. Gutierrez, „Influence of prior austenite microstructure on the transformation products obtained for C-Mn-Nb steels after continuous cooling", ISIJ Int., 39, (1999), No. 6, 583 - 591

30. M. Lin, S.S. Hansen, „Effects of Run-out Table Cooling Profile on the Mechanical Properties of C-Mn-Nb-V-Steels", 37th MWSP, Conference Proceedings, ISS 1996 (XXXIII), 79-88

31. C. Hendricks, W. Rasim, H. Janssen, H. Schnitzer, E. Sowka, P. Tesè, „Inbetriebnahme und erste Ergebnisse der Gießwalzanlage der Thyssen Krupp Stahl AG", Stahl und Eisen, 120, (2000), 61-68

32. B.L. Bramfitt, J.G. Speer, „A Perspective on the Morphology of Bainite", Metall. Trans., 21A, (1990), 817-829

33. D.Q. Bai, S. Yue, T. Maccagno, J.J.Jonas, „Effect of Deformation and Cooling Rate on the Microstructure of Low Carbon Nb-B Steels", ISIJ Intern., 1998, N 4, 371-379

34. R.K. Ray, J.J.Jonas, „Transformation textures in steels", Intern. Mat. Reviews, 35, (1990), N.1, 1-36